EXTENDED KALMAN FILTER APPLICATION IN DIRECT TORQUE CONTROL FOR SPEED ESTIMATION

Anıl BULUT[1], Tarık Veli MUMCU[1*]

[1]Department of Electrical- Electronics Engineering, İstanbul University – Cerrahpaşa, İstanbul, Türkiye

Keywords	Abstract
Direct Torque Control, Extended Kalman Filter, Speed Estimation, Induction Motors.	In this study, in cases where accurate measurements could not be taken, the speed of the asynchronous motor was estimated using the direct torque control method and extended Kalman filter. The switching table, stator flux and electromagnetic moment evaluators, flux and torque controller, which are the components of the direct torque control method, were examined and the output parameters at different switching frequencies were simulated. The loss relationship for different switching frequencies during the application of the extended Kalman filter in direct torque control is discussed.

DOĞRUDAN MOMENT KONTROLÜNDE HIZ TAHMINI İÇIN GENIŞLETILMIŞ KALMAN FILTRESI UYGULAMASI

Anahtar Kelimeler	Öz
Doğrudan Moment Kontrolü, Genişletilmiş Kalman Filtresi, Hız Kestirimi, Asenkron Motorlar.	Bu çalışmada, sağlıklı ölçümlerin alınamadığı durumlarda asenkron motorun, doğrudan moment kontrol yöntemi ve genişletilmiş kalman filtresi kullanılarak hızı kestirilmiştir. Doğrudan moment kontrolü yönteminin bileşenleri olan anahtarlama tablosu, elektromanyetik moment ve stator akı değerlendiricileri, moment denetleyicisi ve akı denetleyicisi incelenerek farklı anahtarlama frekanslarındaki çıkış parametreleri için benzetim çalışması yapılmıştır. Genişletilmiş kalman filtresinin doğrudan moment kontrolünde uygulanması sırasında farklı anahtarlama frekansları için kayıp ilişkisi tartışılmıştır.

[*]İlgili yazar / Corresponding author: tarik.mumcu@iuc.edu.tr, +90-212-404-0300

EXTENDED KALMAN FILTER APPLICATION IN DIRECT TORQUE CONTROL FOR SPEED ESTIMATION

Anıl BULUT[1], Tarık Veli MUMCU[1†]
[1]Department of Electrical- Electronics Engineering, İstanbul University – Cerrahpaşa, İstanbul, Türkiye

Highlights

- Controling of a asynchronous motor by using Direct Torque Control and Extended Kalman Filter
- Analysis of losses for different switching frequency
- Analysis of motor control at different switching frequencies

Purpose and Scope

To analyse direct torque control, which is a common control technique frequently applied to industrial processes in industry such as factories, and production facilities, in presence of the extended Kalman filter for speed estimation as well as to analyse losses based on the switching frequency in presence of extended Kalman filter in direct torque control.

Design/methodology/approach

Simulation studies have been conducted on Direct Torque Control of an asynchronous motor using the extended Kalman filter. An analysis regarding losses based on the switching frequency has been performed.

Findings

Simulations were performed using the classical DTC method and the extended Kalman filter for approximately 6 kHz and 10 kHz switching frequencies. Since classical DTC operates with variable switching frequencies, these values represent the average behavior during the simulation. As a result of these operations, it was observed that the distortions in motor currents and total harmonic distortion increase as the switching frequency decreases. However, high-frequency switching leads to increased switching and energy losses and reduced semiconductor life.

Originality

Direct Torque Control is a method frequently used in industry and the practical use of this method is increasing day by day. The aspects that distinguish this study are the application of the extended Kalman filter in cases where there is no sensor or reliable measurements cannot be made for speed estimation and the harmonic analysis of switching losses for different operating frequencies during this application.

† İlgili yazar / Corresponding author: tarik.mumcu@iuc.edu.tr, +90-212-404-0300

1. Introduction

In the literature, there have been numerous studies on electric motor controls. Considering the control methods, types of motors, and controllers used, the topic of motor control has a broad scope. When examining control methods in general, digital control and vector-based control systems are often encountered. In variable speed control applications of asynchronous motors, two popular methods that provide better performance are direct torque control and field-oriented control (Pimkumwong & Wang, 2018). When these two vector control-based methods are compared, some of the most significant differences between these two leading techniques can be given as, the simpler structure, faster response to requirements, and less dependence on machine parameters for the direct torque control method (Ammar et al., 2018; Okumus et al., 2007).

In the mid-1980s, for asynchronous motor torque control a new control technique was introduced as direct torque (DTC) control by I. Takahashi and T. Noguchi, and as direct self-control by M. Depenbrook. This method has been developed farther by many researchers since 1988 (Tang & Lin, 2010). In this method, the voltage vector of a stator is selected in relation for the difference of the real torque and flux reference. In the topology of DTC, the stator flux and the torque parameters are take into consideration independently and directly, aim to maintain within a specified hysteresis band (Aberkane et al.,, 2018). The advantage of the direct torque (DTC) as a method can be named as the absence of complex transformations and calculations, making it straightforward to implement. It consists of two comparators and a switching table to control the flux and the torque (Gao & Cai, 2015). However, its main disadvantage is the high fluctuations in initial torque values (Mohamed et al., 2015). One approach to prevent fluctuations is to use high-frequency switching drivers. The drawback of this is an increase in electrical power losses and a decrease in the efficiency of the driver (Khazraj et al., 2016). Another approach used to reduce torque fluctuations is the space vector modulation technique (Asif et al., 2017).

One of the most current topics in recent years is sensorless motor control. To increase the overall system reliability and reduce costs, some approaches have been proposed for removing speed and flux sensors in the control of induction motors (Allaoui et al., 2015). While proposed studies in this regard yield good results at nominal speeds, there are still some problems at low speeds. Among all observation-based techniques, the extended Kalman filter (EKF) is efficient for calculating instantaneous states in sensorless motor control (Duvvuri et al., 2018). The quality of the observer in sensorless speed control applications of electric drives plays a significant role, and the observer output parameters are quite sensitive to system parameters (Goswami et al., 2019).

The extended Kalman filter enables dynamic state estimation. EKF calculates the current, flux, and speed values of the induction motor at each step. Thus, the prediction process during the extended Kalman filter method is to linearize non-linear transformations and calculations using the Jacobian matrix to reduce noise effects and modeling errors. Lastly, the dynamic state analysis algorithm allows the calculation of the dynamic state (Djellouli et al., 2011).

Within the many applications in classical DTC where switching frequency is inherently variable, it is not always feasible to increase the average operating frequency due to limitation of semiconductors during the switching before they reach their thermal limits. To illustrate this issue high-power drives can be given as a good application case, where the operating frequency has to be limited as to the used semiconductors and their cooling systems (Karlovsky et al., 2020). DTC as an approach and within its protocol, an increase in the operating frequency and the pattern of power devices are varying, higher losses for the switching become visible, resulting in a decrease in overall efficiency (Carlos et al., 2025). Moreover, the aim of this article is to provide an understanding for the relationship between switching frequency and losses in direct torque control in presence of extended Kalman filter for speed estimation.

2. Direct Torque Control

One main objective in DTC is the accurate control of the stator magnetic field and the electromagnetic torque through the selection of appropriate stator voltage vectors (Wu & Narimani, 2017). The values of i_α, i_β, V_α, and V_β are calculated using the measured current at the drive output and the voltage value at the DC bus of the drive. Using these values, the required stator magnetic fields and electromagnetic torque are determined. Error signals are generated by comparing these required values with reference values. Based on the error signals, appropriate selections are made from the vector switching table to capture the reference value, ensuring that the drive switches are oriented accordingly. Figure 1 illustrates the general structure of DTC. As the figure sets forth, DTC as an approach can be considered in three sections.
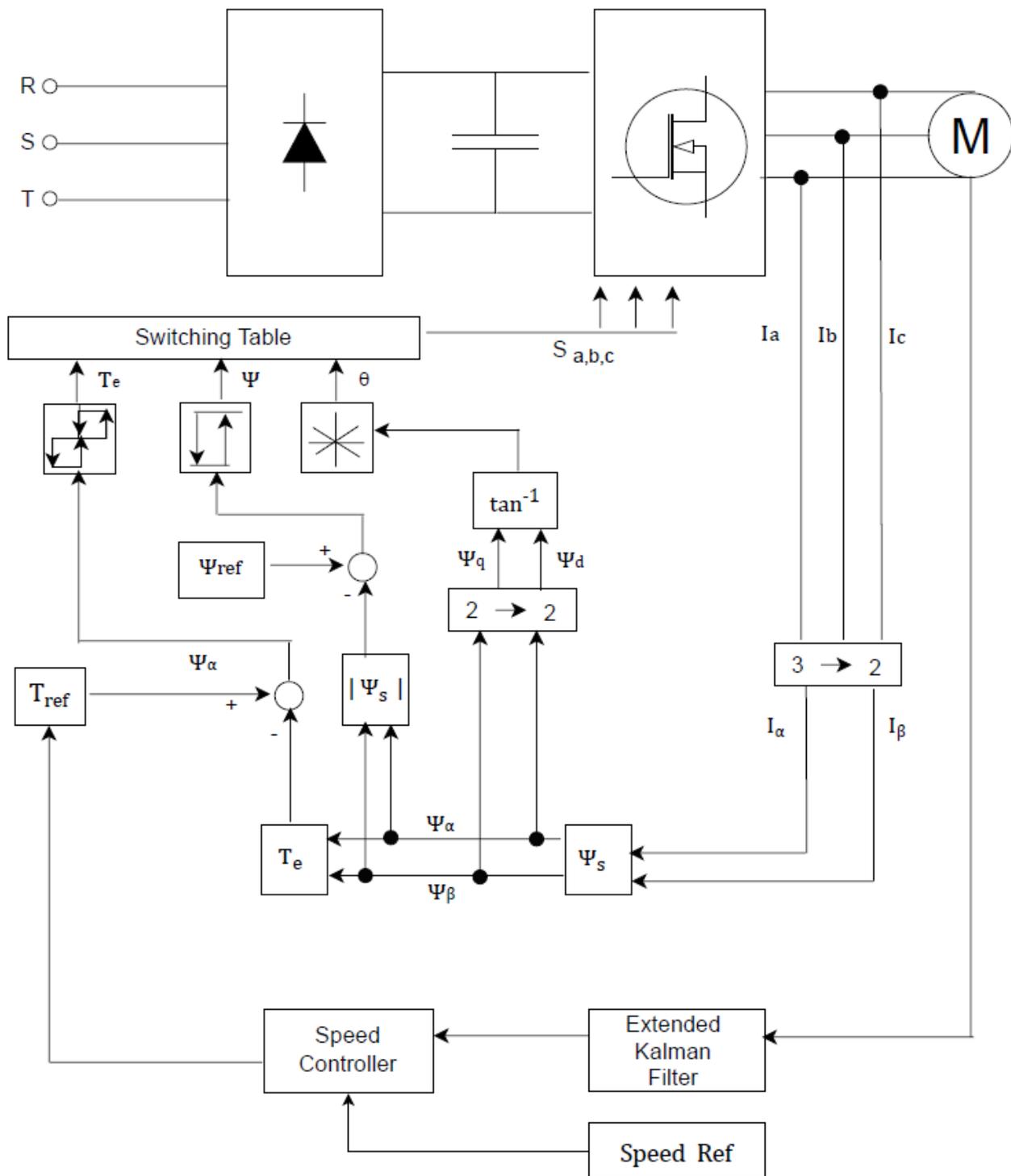
Figure 1. General Structure of Direct Torque Control

2.1 Sections in Direct Torque Control System

2.1.1 Flux and Torque Controller

When an asynchronous electrical motor system controlled with DTC, For the torque and the stator flux the presented references are validated with their current values and the difference is calculated as error or error ratio. This error signal is sent to the comparators seen in Figure 1. In traditional direct torque control methods, the errors in torque and flux are each attempted to be limited within a certain band range. The interval of these band limits is generally considered as $2\Delta\varphi_s$, $2\Delta T_e$ (Reddy & Sheker, 2014). Figure 2 provides the structure of the flux controller. The error ratio calculated by comparing the existing flux and reference flux is sent to the switching table, ensuring the selection of the appropriate switching.

2.1.2 Switching Table

The stator magnetic flux position can be represented vectorally in the α-β axis as well as the magnetic flux position can be considered in six different regions. Therefore, The appropriate choice of the vector(s) necessary to stay within the hysteresis band range is realized by making appropriate switches, and the aim is to bring the torque and flux values within error band of the desired values. Furthermore, with the help of the hysteresis comparators and the region data related to the stator flux, the requested voltage vector is chosen on the related table. The tables for voltage vectors are given as in follow on Table 1 and Table 2. Thus, electrical motor drive triggers now can be controlled at this step using vectors V_1, V_2, ..., V_7 on Table 1 and Table 2. In other words, these tables below show the switching that needs to be made based on error conditions from flux and torque controllers. As an example, if the value "1" comes from the torque and the flux value regulators and the second region is arranged, the appropriate switching will be realized by the V_3 vector (Patra, N., 2013).

Table 1: Switching Based on Flux and Torque Controller

B_ϕ	bt	S_1	S_2	S_3	S_4	S_5	S_6
	1	V_2	V_3	V_4	V_5	V_6	V_1
1	0	V_7	V_0	V_7	V_0	V_7	V_0
	-1	V_6	V_1	V_2	V_3	V_4	V_5

Table 2: Switching Based on Flux and Torque Controller

B_ϕ	bt	S_1	S_2	S_3	S_4	S_5	S_6
	1	V_3	V_4	V_5	V_6	V_1	V_2
0	0	V_0	V_7	V_0	V_7	V_0	V_7
	-1	V_5	V_6	V_1	V_2	V_3	V_4

2.1.3 Electromagnetic Torque and Stator Flux Evaluators

The electromagnetic torque stator flux and evaluators are responsible for calculating the torque and the flux linkage values in classical DTC. Firstly, the V_{abc} used in the motor supply is expressed as $V_{\alpha\beta}$ using the transformation formulae. The same transformation is also valid for the current used in calculations of the electromagnetic torque and the flux. Subsequently, the new expressions for the voltage and the current, the flux and torque estimations, will define a significant sector used in the drive. Figure 2 illustrates the calculation of existing flux, torque, and angle values using voltage and current values associated with the motor. These values will be sent to the hysteresis operator and the switching table for evaluation(Patra, N., 2013).
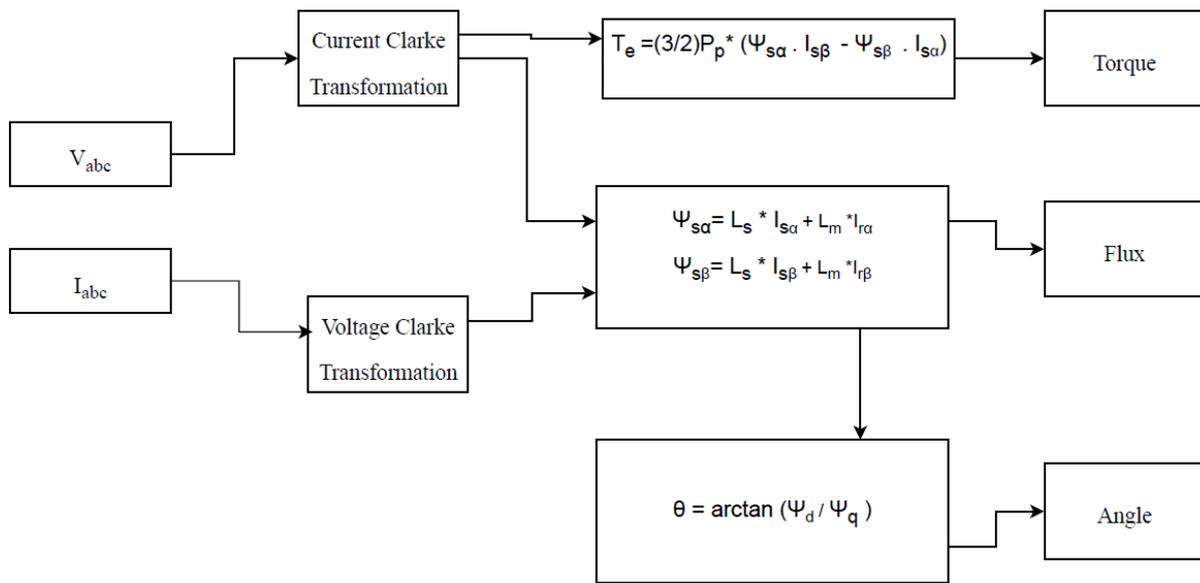
Figure 2: Representation of Flux, Torque, and Angle Calculations

3. Kalman Filter

Kalman Filter is a filter that can predict the state of a dynamic system represented by a state-space model based on the previous information of the model and output information. Despite its filtering feature like traditional predictors, the Kalman filter is powerful and capable of predicting unmeasurable states of the system.

In a conventional Kalman filter, the application process can be given as follows:

The initial state prediction value is used for the next state value which is calculated based on the system model values and the covariance of system noise. The Kalman gain is found by using the system model value, the calculated next state value, and the covariance values of measurement noise, which are specific to the Kalman filter. The Kalman gain is used to obtain the optimal state by considering the calculated state value, the initial state value, and the measured data. While Kalman filters provide successful results in linear systems, non-linear systems may not achieve the desired accuracy. For non-linear systems, extended Kalman filters (EKF), which can provide more accurate results, are preferred. Since the asynchronous motor model is non-linear, it is more suitable to use an extended Kalman filter. Here, stochastic continuous time should be expressed in discrete form to adapt to the structure of the extended Kalman filter. The math model of the system is linearized using the Jacobian in EKF. The noise, measurement, and state covariance matrices are determined, and the system attempts to make an optimal estimation related to the state as previously described. Figure 3 shows the flow diagram used in the operation of the Kalman filter. The Kalman filter uses the initial state to calculate the predicted state, and then the current and most appropriate state value is estimated considering the measurement values and the predicted state (Alsofyani et al., 2016).
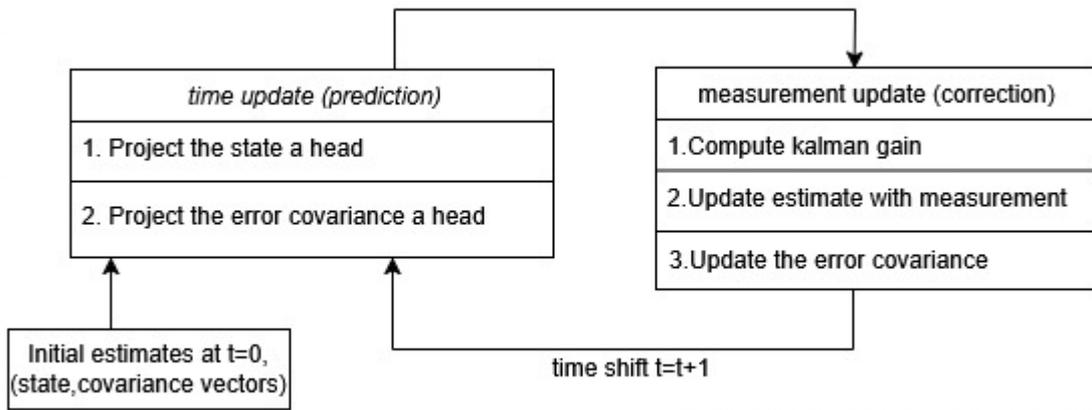
Figure 3: Kalman Filter Flow Diagram

4. Simulation Results

Direct torque control has a shorter cycle time and a faster response to generated changes compared to field-oriented control due to having fewer mathematical transformations. In brief, to summarize direct torque control: The three-phase current and voltage values on the motor feeding side are measured. The measured voltage and current values are subjected to a Clarke transformation for easier calculation and are defined in the stator-fixed coordinate system. After the Clarke transformation, the obtained values are used to calculate the current torque, flux, and flux angle through the stator electromagnetic torque evaluator. The current torque and flux values are validated with the desired values to provide the necessary error(s). These error(s) are sent to the torque and flux evaluators. At this point, an evaluation is made regarding whether to increase, decrease, or maintain the current torque or flux, and a signal is sent to the switching table. Consequently, The table evaluates the incoming signals and the flux region to determine the vector selection that the drive should apply for the switching. The switches in the drive take positions based on the data received from the switching table.

In this study, the direct torque control method in the presence of an extended Kalman filter at different switching frequencies were observed as results. In general, it was observed that as the switching frequencies increased, the fluctuations in torque decreased. The simulation results of the study are as follows:
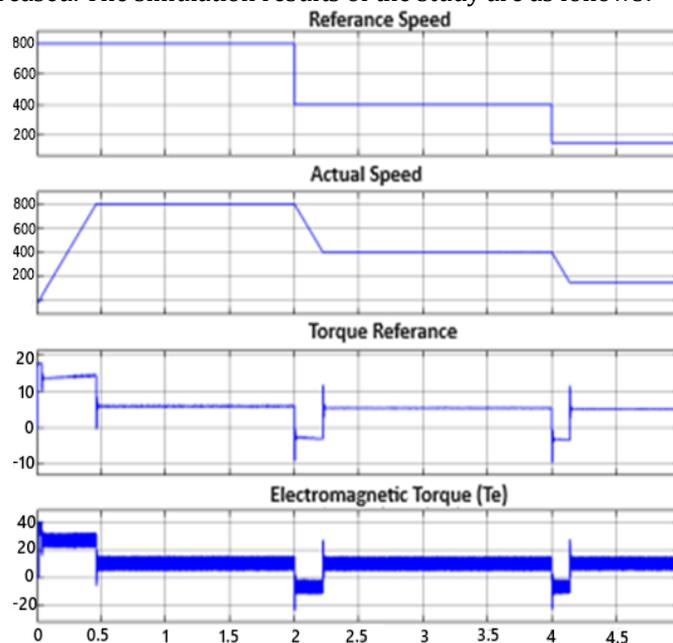

Figure 4: Direct Torque Control - Torque Reference and Actual, Speed Reference and Actual (10 kHz)

In Figure 4, the reference speed and the electromagnetic torque value, actual speed and torque reference for a switching frequency of 10 kHz are given. The reference speed is gradually reduced and it is seen that the actual speed of the motor follows the reference speed value. The torque reference value is created by the speed controller and sent to the system as a reference, and the electromagnetic torque graph for a switching frequency of 10 kHz are compatible and can be observed in Figure 4.
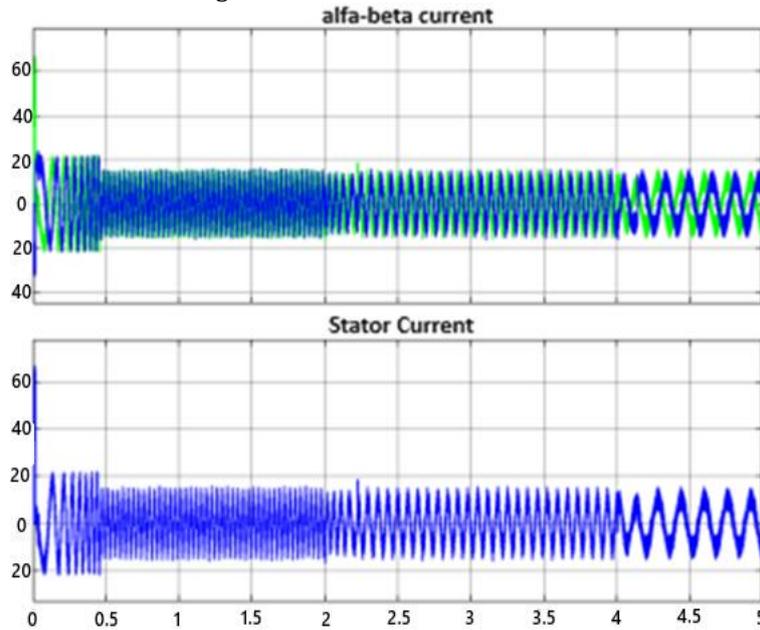
Figure 5: Direct Torque Control Line Currents (10 kHz)

In Figure 5, the current value formed in the windings of the motor and counter part in the alpha – beta axis are observed for the same switching frequency and reference input, like in Figure 4.The stator currents are measured according to the speed reference in Fig 4. It is seen that the frequencies of the stator currents decrease as the reference speed decreases. While the speed value was 800 rpm at the beginning, it decreased to 400 rpm in the 2nd second and 200 rpm in the 4th second. As a result, it is seen that the frequency of the motor stator current decreases and becomes visible.
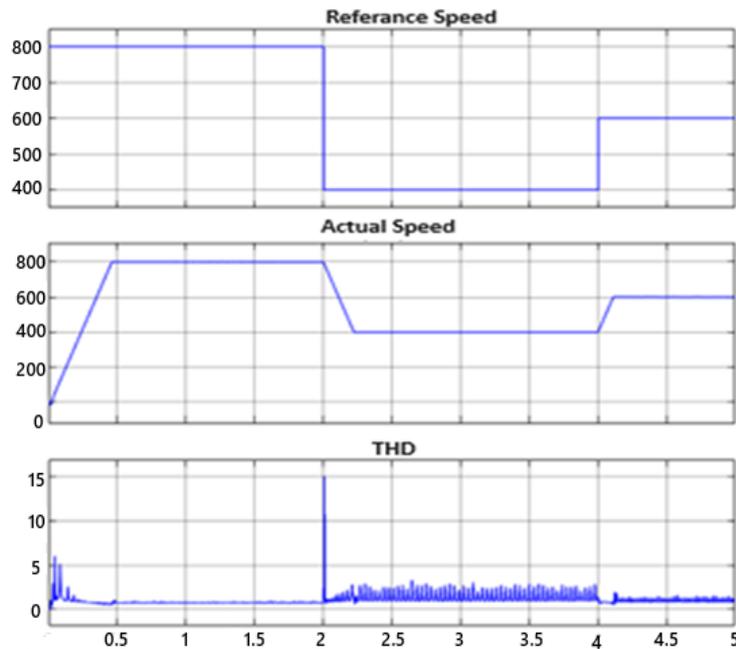
Figure 6: Direct Torque Control Line Currents THD Analysis (10 kHz)

In Figure 6, the total harmonic distortion for the given reference value at a switching frequency of 10 kHz is simulated. The total harmonic distortion occurring in the system at different speed values is examined. When the speed reference harmonic relationship is examined; it is seen that the harmonic distortion is at its lowest value

between 0-2 seconds. It is determined that the distortions increase when the reference speed value is reduced to 400 rpm between the 2nd and 4th seconds and finally, after the 4th second, when the reference value is at 600 rpm, there is a slight decrease in THD.
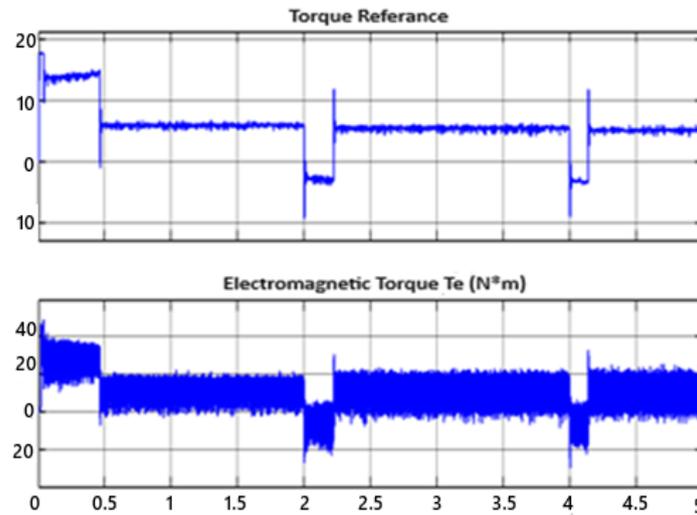

Figure 7: Direct Torque Control - Torque Reference and Actual (6 kHz)

In Figure 7, the reference and actual electromagnetic torque values given to the driver in a system controlled with direct torque are shown. Using the same system and load, the switching frequency is selected to a lower value which is 6 kHz. Here, it is seen that there are more fluctuations in the torque reference compared to the first case.
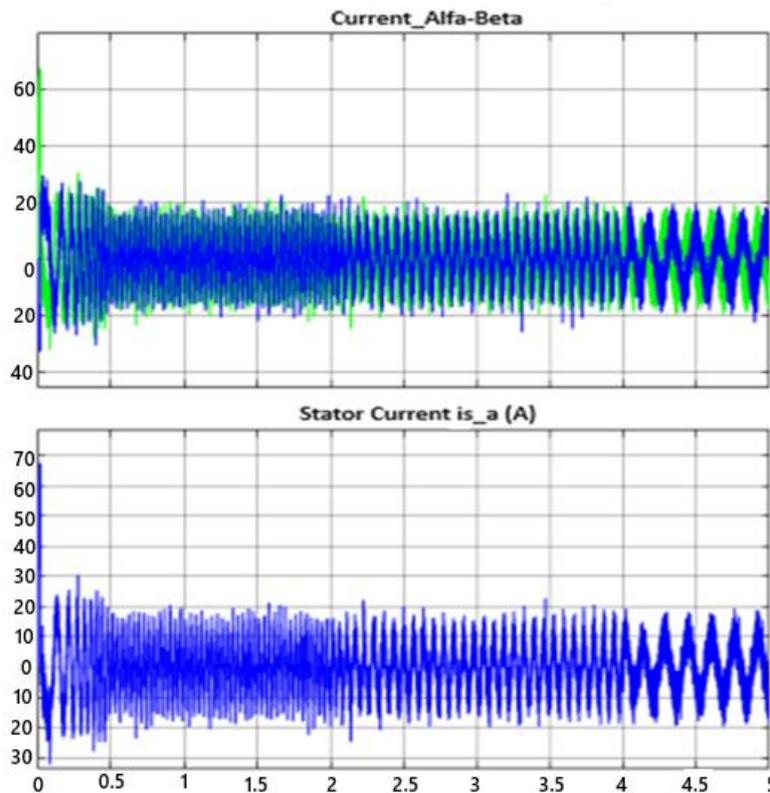

Figure 8: Direct Torque Control Line Currents (6 kHz)

The same system with similar reference values is simulated and examined in terms of motor currents when the switching frequency is set to 6 kHz in Figure 8. The motor currents is seen as current phase (A) and the current on the alpha-beta frame. When the simulation is compared to 10 kHz switching frequency, the fluctuations on the

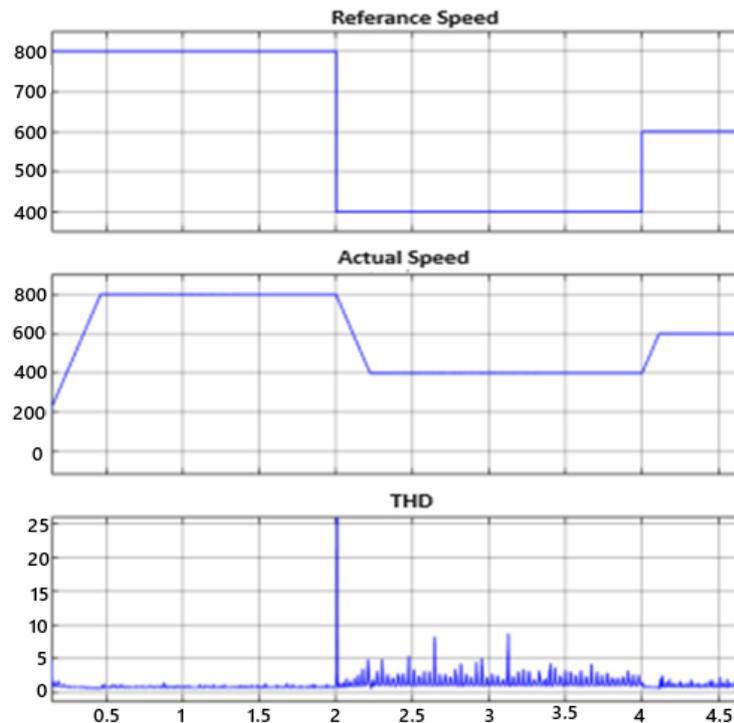motor currents are higher in 6 kHz switching frequency.

Figure 9: Direct Torque Control Line Currents THD Analysis (6 kHz)

In Figure 8-9, the line currents and total harmonic distortion can be observed. As seen in Figure 8-9, as the switching frequency decreases, distortions in motor currents and an increase in total harmonic distortion are observed.

5. Conclusion

In this study, the effect of switching frequency on losses for the DTC controlled asynchronous motor with extended Kalman Filter is considered. When different average switching frequencies (6 kHz and 10 kHz represent average switching frequencies obtained via hysteresis tuning DTC switching remains variable in time) are compared, it is seen that motor currents have more fluctuations under a lower average switching frequency which is around 6 kHz in classical DTC, and it can be observed that total harmonic distortion is also higher than at 10 kHZ switching frequency. However, in the case where 10 kHZ switching frequency is used, a higher average switching frequency, obtained through narrower hysteresis bands in classical DTC, leads to increased switching and energy losses in semiconductors, shortening of their life and heating. As a result, high switching frequency in DTC improves motor performance but more switching loss occurs in the drive.

Ultimately, a decreased switching frequency causes more frequent current ripples for the line currents of the induction motor. These increased current ripples lead to greater heating in the stator resistances, resulting in additional losses. Moreover, the high-frequency voltage vectors generate continuously alternating magnetic fields, which contribute to increased eddy current losses.

Conflict of Interest

No conflict of interest was declared by the authors.

References

Aberkane, H., Sakri, D., & Rahem, D. (2018). Comparative study of different variants of direct torque control applied to induction motor. 2018 9th International Renewable Energy Congress (IREC), 1–6. https://doi.org/10.1109/IREC.2018.8362484.

Alsofyani, M and Idris, N.R.N. "Lookup-Table-Based DTC of Induction Machines With Improved Flux Regulation and Extended Kalman Filter State Estimator at Low-Speed Operation," in IEEE Transactions on Industrial Informatics, vol. 12, no. 4, pp. 1412-1425, Aug. 2016, doi: 10.1109/TII.2016.2571682.

Allaoui, S., Chaada, K., Laamari, Y., & Athamena, B. (2015). Induction motor state estimation using tuned extended Kalman filter. 4th International Conference on Electrical Engineering (ICEE), Boumerdes, Algeria, pp. 1-5, doi: 10.1109/INTEE.2015.7416676.

Ammar, A., Kheldoun, A., Metidji, B., Talbi, B., Ameid, T., & Azzoug, Y. (2018). An experimental assessment of direct torque control and model predictive control methods for induction machine drive. International Conference on Electrical Sciences and Technologies in Maghreb (CISTEM), Algiers, Algeria, pp. 1-6, doi: 10.1109/CISTEM.2018.8613419.

Asif, M. J., Shahbaz, T., Hassan, S. U., & Rizvi, S. T. H. (2016). Mathematical modelling of 3-phase induction motor to study the torque vs. speed characteristics using MATLAB Simulink. 19th International Multi-Topic Conference (INMIC), Islamabad, Pakistan, pp. 1-7, doi: 10.1109/INMIC.2016.7840144.

Carlos, A. R., Parra, M., Aguilar, G. M., & Gonzallez-Diaz, V. R. (2025). Comparison of induction machine drive control schemes on the distribution of power losses in a three-level NPC converter. Machines, 13(3), 227. https://doi.org/10.3390/machines13030227.

Depenbrock, M. (1988). "Direct self-control (DSC) of inverter-fed induction machine," in IEEE Transactions on Power Electronics, vol. 3, no. 4, pp. 420-429, Oct. 1988, doi: 10.1109/63.17963.

Djellouli, T., Moulahoum, S., Boucherit, M., & Kabache, N. (2011). Sensorless direct torque control for saturated induction motor using extended Kalman filter. International Aegean Conference on Electrical Machines and Power Electronics and Electromotion, İstanbul, Türkiye, 190–194, doi: 10.1109/ACEMP.2011.6490593.

Duvvuri, S. S. S. R., Dangeti, L. K., Garapati, D. P., & Meesala, H. (2018). State estimation for wound rotor induction motor using discrete-time extended Kalman filter. International Conference on Power, Instrumentation, Control and Computing (PICC), Thrissur, India, pp. 1-6, doi: 10.1109/PICC.2018.8384810.

Gao, S., & Cai, Y. (2015). Torque ripple minimization strategy for direct torque control of induction motors. Third International Conference on Intelligent Networks and Intelligent Systems, Shenyang, China, 2010, pp. 148-151, doi: 10.1109/ICINIS.2010.82.

Goswami, G., & Thakura, P. R. (2019). A speed and flux observer using square root cubature Kalman filter for induction motor drive. 2019 International Conference on Vision Towards Emerging Trends in Communication and Networking (ViTECoN), 1–6. https://doi.org/10.1109/ViTECoN.2019.8899687

Karlovsky, P., Lipcak, O., & Bauer, J. (2020). Iron loss minimization strategy for predictive torque control of induction motor. Electronics, 9(4), 566. https://doi.org/10.3390/electronics9040566

Khazraj, H., Silva, F., & Bak, C. L. (2016). A performance comparison between extended Kalman filter and unscented Kalman filter in power system dynamic state estimation. 2016 51st International Universities Power Engineering Conference (UPEC), Coimbra, Portugal, pp. 1-6, doi: 10.1109/UPEC.2016.8114125.

Mohamed, C., Golea, A., & Bencholuia, M. T. (2015). Implementation of a predictive DTC-SVM of an induction motor. 4th International Conference on Electrical Engineering (ICEE), Boumerdes, Algeria,pp. 1-4, doi: 10.1109/INTEE.2015.7416733.

Okumus, H. I., & Aktaş, M. (2007). Direct torque control of induction machine drives using adaptive hysteresis band for constant switching frequency. IEEE International Electric Machines & Drives Conference, Antalya, Türkiye, 1762–1767, doi: 10.1109/IEMDC.2007.383697.

Patra, N. (2013). Study of induction motor drive with direct torque control scheme and indirect field oriented control scheme using space vector modulation [Master's thesis, National Institute of Technology, Rourkela].

Pimkumwong, N., & Wang, M. (2018). Direct torque control of three-phase induction motor based on constant voltage per frequency control with simple controller. Proceedings of the 2018 International ECTI Northern Section Conference on Electrical, Electronics, Computer and Telecommunications Engineering (ECTI-NCON), 15–20. https://doi.org/10.1109/ECTI-NCON.2018.8378273.

Reddy, D. B., & Sheker, C. V. (2014). Direct torque controlled four-quadrant induction motor drive. The International Journal of Engineering and Science (IJES), 6–14 https://theijes.com/papers/ICIEEE/B06014.pdf.

Takahashi, I. and Noguchi, T. (1986) "A New Quick-Response and High-Efficiency Control Strategy of an Induction Motor," in IEEE Transactions on Industry Applications, vol. IA-22, no. 5, pp. 820-827, Sept. 1986, doi: 10.1109/TIA.1986.4504799.

Tang, Y., & Lin, G. (2010). Direct torque control of induction motor based on self-adaptive PI controller. 5th International Conference on Computer Science & Education, Hefei, China, pp. 1230-1234, doi: 10.1109/ICCSE.2010.5593448.

Wu, B., & Narimani, M. (2016). Control of induction motor drives (2nd ed.). Wiley-IEEE Press.